Langmuir

Letter

pubs.acs.org/Langmuir

An Electrochemically Controlled Microcantilever Biosensor

Yoshihiko Nagai,[†] Jorge Dulanto Carbajal,[‡] John H. White,[§,⊥] Robert Sladek,[†,∥,⊥] Peter Grutter,[‡] and R. Bruce Lennox[#,*]

[†]Research Institute of the McGill University Health Centre, 2155 Guy Street, Montréal, Québec H3H 2R9, Canada

[‡]Department of Physics, McGill University, 3600 Rue University, Montréal, Québec H3A 2T8, Canada

[§]Department of Physiology, McGill University, 3655 Promenade Sir William Osler, Montréal, Québec H3G 1Y6, Canada

[∥]Department of Human Genetics, McGill University, 740 Avenue Dr. Penfield, Montréal, Québec H3A 0G1, Canada

[⊥]Department of Medicine, Royal Victoria Hospital, 687 Pine Avenue West, Montréal, Québec H3A 1A1, Canada

[#]Department of Chemistry and FRQNT Centre for Self Assembled Chemical Structures, McGill University, 801 Sherbrooke Street West Montréal, Québec H3A 2K6, Canada

ABSTRACT: An oligonucleotide-based electrochemically controlled gold-coated microcantilever biosensor that can transduce specific biomolecular interactions is reported. The derivatized microcantilever exhibits characteristic surface stress time course patterns in response to an externally applied periodic square wave potential. Experiments demonstrate that control of the surface charge density with an electrode potential is essential to producing a sensor that exhibits large, reproducible surface stress changes. The time course of surface stress changes are proposed to be linked to an electrochemically mediated competition between the adsorption of solution-based ions and the single- or double-stranded oligonucleotides tethered to the gold surface. A similar potential-actuated change in surface stress also results from the interaction between an oligonucleotide aptamer and its cognate ligand, demonstrating the broad applicability of this methodology.

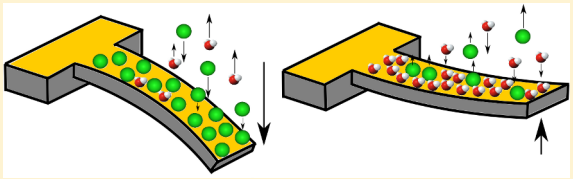

INTRODUCTION

Nanoscale sensors, which can rapidly provide label-free biomarker detection with high sensitivity, have been explored for application to low-cost point-of-care diagnostics, biological warfare agent detection, drug-discovery platforms, and observations of single-molecule biochemical processes in real time. Most nanoscale sensor systems transduce surface stress changes using mechanical devices[1−6] or conductance using field-effect transistor concepts.[7,8] In both methods, the largest signals that result from a specific binding event are generated by changes in surface charge density, leading to changes in stress detected by microcantilever (cantilever) sensors[9−11] or changes in the conductivity of nanowires.[7,8] These transduction mechanisms point to the delicate balance between the dual role of the sensor surface which serves as both a support for the functionalization chemistry and as a transducer for biochemical recognition events. Covering the entire sensor surface with (bio)chemical receptors will, however, often reduce charge density changes close to the surface and thus will reduce the magnitude of an analytical signal. The magnitude of the analytical signal can also be compromised by surface contamination, and time-dependent contamination can lead to apparent aging of the sensor.

Although many cantilever systems that detect biological targets have been reported,[1−6] applications have been limited by problems with both the reproducibility and magnitude of the sensor signal. Given that understanding the origin of signal (surface stress) generation is critical to solving these measurement problems, a number of factors contributing to stress changes have been identified or modeled in the case of gold-coated cantilevers. Factors intrinsic to the coating on the gold, including both attractive and repulsive intermolecular interactions[5,12,13] and configurational entropy changes,[14] have been described as contributors to cantilever-based surface stress measurements. The resulting experimental challenges, including poor signal-to-noise ratios, cantilever-to-cantilever variation, and sensitivity to conditions such as temperature and sample constituents, have led to elegant engineering approaches that increase the precision and/or accuracy of surface stress measurements. These engineering approaches include the simultaneous measurements of multicantilever arrays and differential measurements that reject common mode noise (reviewed in refs 15 and 16).

Although many factors contribute to surface stress changes in a cantilever biosensor experiment, understanding and controlling the relative importance of these factors is difficult and their concomitant deconvolution has generally proven to be intractable. However, the surface charge density has been identified as a dominant factor in determining the deflection of metal-coated cantilevers[9−11,13] and can be orders of magnitude larger than the factors associated with the surface coating itself.[13] Surface stress has been shown to be sensitive (up to 1 N m/C) and is directly proportional to the surface charge density.[17] Changes in the applied potential near the potential of

Received: March 14, 2013
Revised: June 21, 2013
Published: July 10, 2013

   dx.doi.org/10.1021/la400975b | *Langmuir* 2013, 29, 9951−9957

zero charge (PZC), in the presence of either adsorbing (Cl^-, Br^-) or nonadsorbing electrolyte (ClO_4^-), lead to large changes in surface stress.[17] We have thus sought to develop a robust methodology where the principal measurement is the change in the surface stress signal and its temporal features as a function of an applied potential, both in the absence and presence of an analyte of interest. By building on our prior experience[13,18,19] and that of others,[20,21] we have explored the use of the electrochemical control of gold-coated cantilevers. We demonstrate that programmed square wave potential changes applied to nucleic acid-derivatized cantilevers yield characteristic time-dependent surface stress signatures that are related to the quantity of surface-tethered nucleic acid both before and after hybridization with complementary oligonucleotide or after ligand capture by an oligonucleotide aptamer.

EXPERIMENTAL SECTION

Cantilever Preparation. Silicon cantilevers (type CSC12 tipless, MikroMasch, Bulgaria) are coated with titanium by thermal evaporation to a depth of 2 nm at a rate of 0.04 nm/s and with gold to a depth of 100 nm at a rate of 0.14 nm/s at a pressure $<5.0 \times 10^{-6}$ Torr and 130 ± 20 °C (Thermionics model VE90 vacuum evaporator, Thermionics Laboratories, USA). A layer of Apiezon wax (Apiezon Wax W, APWK, Apiezon, USA) dissolved in trichloroethylene (TCE) (Fisher Scientific, USA) is deposited on a portion of the gold surface to yield a gold electrode surface area of 1.0 mm^2. Gold-coated cantilevers are then electrochemically cleaned via repetitive electrochemical cycling (−0.8 to 1.3 V vs saturated Ag/AgCl) in $KClO_4$ solution (50 mM) at a scan rate of 20 mV/s until a repeatable voltammogram is obtained (BASi CV-50W voltammetric analyzer, Bioanalytical Systems, Inc., USA). Cleaning of the cantilever surface in this manner was performed immediately before each experiment.

Electrochemical Methods. The cleaned gold-coated silicon cantilever (Figure 1A) was clamped with a copper clip to a Kel-F rod and partially immersed in a buffer containing TN buffer (10 mM Tris-HCl, 50 mM NaCl, pH 7.4) in an argon-saturated 6 mL homemade electrochemical cell equipped with an Ag/AgCl (saturated) reference electrode and a 1-mm-diameter platinum wire counter electrode (both from Bioanalytical Systems, Inc., USA). The potential of the gold-coated cantilever was controlled by the potentiostat. Cantilever bending was measured by optical deflection using a 10 mW laser diode module (Hitachi HL6334MG, Japan) and a position-sensitive detector (PSD) (On-Trak Photonics, USA). The observed deflections were converted to stress values based on the stiffness of the cantilever (determined by measuring its resonance frequency and corresponding quality factor using thermoacoustic methods[22−24]). The cantilever deflection measurements use a protocol involving a periodic square wave potential of ±200 mV and a standard switching interval (t_{cycle} = 10 min). The potential window of ±200 mV was based on the potential range of Cl^- adsorption on Au(111).[25,26]

Blocking of the Gold Surface with 6-Mercapto-1-hexanol (MCH). After deflection measurements were performed on the clean gold-coated cantilever, it was incubated for 1 h in a 1.0 mM ethanolic solution of MCH (Fisher Scientific, USA). Before an additional deflection measurement was performed, the cantilever was rinsed three times alternately with ethanol and 50 mM NaCl. Deflection measurements were performed by initially holding the surface potential at V_{appl} = −200 mV for 2 min in TN buffer and then switching to +200 mV.

DNA Oligonucleotide Functionalization and Hybridization Assays. Experiments were performed using a 25-mer thiolated single-strand oligonucleotide (probe-oligo) with sequence 5′-HS-SC_6-TCGGATCTCACAGAATGGGATGGGC-3′ (IDT Technology, USA) diluted to a final concentration of 100 μM in 40 μL of TE buffer (10 mM Tris-HCl, 5 mM EDTA, pH 8.0). The probe-oligo is desalted by incubating with 0.1 M dithiothreitol (DTT) (Sigma-Aldrich, USA) for 30 min and then purified using a NAP-5 column

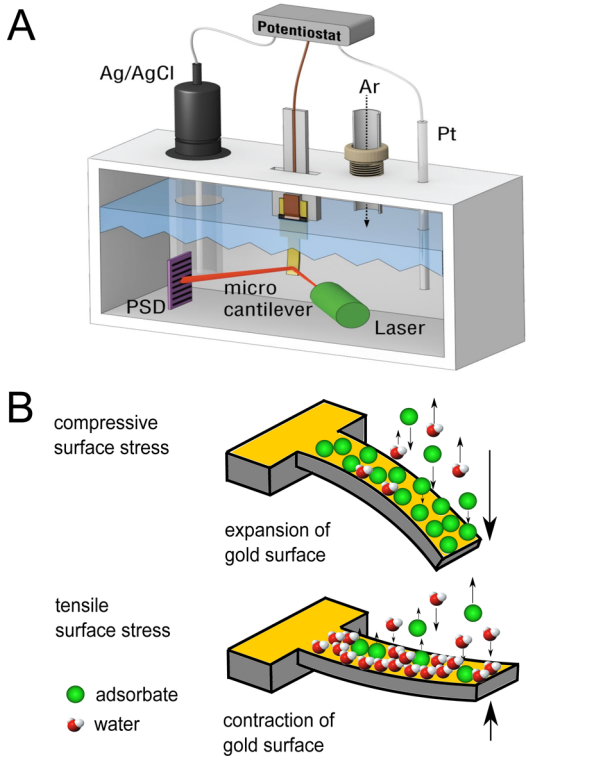

Figure 1. Schematic diagram of the electrochemical cell and electrochemically induced surface stress. (A) The silicon cantilever coated with evaporated titanium (2 nm) and gold (100 nm). Insulating Apiezon wax selectively coats areas of the cantilever to control the area of the gold-coated cantilever surface which is exposed to the electrolyte solution. The cantilever working electrode is held in the electrochemical cell using a copper plate spring. An Ag/AgCl (saturated) reference electrode and a platinum wire counter electrode are used. In each experiment, the gold surface is electrochemically cleaned in 50 mM $KClO_4$ (see Experimental Section) immediately before the measurement. The cantilever deflection is measured optically. (B) Deflections are induced by changes in the surface charge density, mediated by adsorption and desorption of ions in response to changes in the applied potential. The first schematic shows the induction of compressive stress (expansion of the gold surface) by the adsorption of component(s) of the electrolyte. The second schematic shows the induction of tensile stress (contraction of the gold surface) when adsorbed ions are released from the gold surface.

filter (GE Healthcare, U.K.) with TN buffer. The purity of the filtered probe-oligo solution was confirmed with ESI mass spectrometry. In all experiments, the concentration of the probe-oligo was adjusted to a final concentration of 3.0 μM. Two methods are used to functionalize the cantilever with thiolated oligonucleotides. In the single-step functionalization procedure, the gold-coated cantilever is incubated in the probe-oligo solution for 30 min and then rinsed three times with Milli-Q water (resistivity <18 MΩ cm, Millipore, USA). In the multistep functionalization procedure, the clean gold-coated cantilever was repetitively incubated in the probe-oligo solution for 5 min periods. The cantilever is subjected to a ±200 mV square wave potential regime (t_{cycle} = 10 min; three cycles) after each incubation. The surface-tethered probe-oligo is hybridized with a complementary 25-mer oligonucleotide (target-oligo) whose sequence is 5′-GCCCATCCCATTCTGTGAGATCCGA-3′ (IDT Technology, USA) to a final concentration of 3.0 μM in 100 μL of TE buffer. Hybridization of the target-oligo to the probe-oligo is performed by incubating the functionalized gold-coated cantilever in 3.0 μM target-oligo in TE buffer solution at 48 °C (the calculated melting temperature of the oligonucleotide sequence) for 15 min and cooling to room temperature to avoid mismatch binding. Following hybrid-

dx.doi.org/10.1021/la400975b | Langmuir 2013, 29, 9951−9957

ization, the gold-coated cantilever is thoroughly rinsed three times with Milli-Q water to remove any physisorbed target-oligo from the gold surface.

Oligonucleotide Aptamer-Ligand Binding Assay. Experiments are performed using a 24-mer thiolated single-strand oligonucleotide aptamer (probe-aptamer) with sequence 5′-HS-SC_6-GATCGAAACG-TAGCGCCTTCGATC-3′ (IDT Technology, USA) diluted to 100 μM in 40 μL of TE buffer. This sequence has been previously shown[27] to bind to L-Arm (L-argininamide dihydrochloride, Sigma-Aldrich, USA) with a dissociation constant of 220 μM and a melting temperature of 42 °C. The gold-coated cantilever is functionalized with desalted probe-aptamer so that its stress pattern response matches that of the ca. 12% surface coverage of probe-oligo obtained by the multistep functionalization method. The aptamer binding ligand, L-Arm, is diluted to a final concentration of 1.0 mM with TN buffer and adjusted to pH 7.0. After the deflection of the probe-aptamer-coated gold-coated cantilever is measured, the cantilever is incubated in an L-Arm solution for 30 min and thoroughly rinsed with Milli-Q water three times at room temperature.

Measurement of Oligonucleotide Surface Coverage. Following the completion of a cantilever deflection experiment, a gold-coated cantilever is incubated in a 1.0 mM ethanolic solution of 12-ferrocenyl-1-dodecanethiol ($Fc(CH_2)_{12}SH$; Fc = (η^5-C_5H_5)Fe(η^5-C_5H_4)) for 1 min. $Fc(CH_2)_{12}SH$ occupies available gold sites on the cantilever surface.[28] The signature redox peaks of surface-confined $Fc(CH_2)_{12}SH$ are determined by cyclic voltammetry (0 to 700 mV vs saturated Ag/AgCl; scan rate 20 mV/s) in 0.1 M $NaClO_4$. The coverage of $Fc(CH_2)_{12}SH$ is determined from the charge associated with the oxidation peak in the cyclic voltammogram. The gold electrode area is assumed to be equal to its geometric area.

RESULTS AND DISCUSSION

An electrochemical cantilever cell (Figure 1A) was used to examine the relationship between applied potential (V_{appl}) and the cantilever deflection in the presence of ions (Cl^-) that are known to adsorb to gold in a potential-dependent manner (Figure 1B). These studies use an applied potential range over which Cl^- adsorption changes.[25,26,29] Holding V_{appl} at three different potentials in this range (+200, −50, and −200 mV) for 2 min (Figure 2A) results in different quantities of Cl^- adsorption and surface charge density values.[25,26] However, the release of the potential from fixed to open circuit conditions and monitoring the ensuing cantilever deflection as a function of the changing open circuit potential (OCP) reveals a little-appreciated challenge in the use of cantilevers as sensors: very large surface stress changes (σ; up to 100 mN/m) occur as the open circuit potential moves toward the equilibrium rest potential value of the electrode (Figure 2A). Because the surface charge density (and thus surface stress) of the gold-coated cantilever is controlled by the electrode potential and the nature of the adsorbates (whose affinity for the electrode surface is invariably potential dependent[9−11]), only fixed potential conditions can ensure stable and reproducible values of surface stress with time. Operating at the OCP effectively reduces the cantilever to serving as a complex voltmeter. Many factors determine the OCP of an electrode near its potential of zero charge, including the Nernstian potential of the solution and the speciation and quantity of adsorbates, including those making up the buffer and electrolyte. Changes in the adsorbate species and/or their quantity lead to a change in the OCP and thus the extent (and direction) of cantilever deflection.

To evaluate the contribution of surface charge density changes to the cantilever deflection, we compared the changes in surface stress resulting from the application of a series of ±200 mV potential steps to a clean gold-coated cantilever and one coated with 6-mercapto-1-hexanol (MCH) (Figure 2B). A

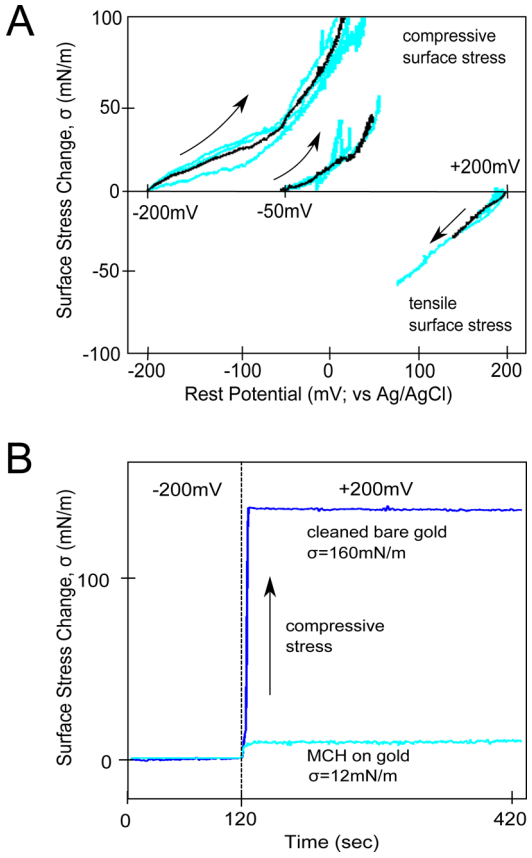

Figure 2. Electrochemical control of microcantilever surface stress changes. (A) Relationship between the surface stress change and the applied potential of the gold surface. The potential of the cleaned gold-coated cantilever was held at three values (−200 mV, −50 mV and +200 mV) for 2 minutes and then released to OCP (open circuit potential) conditions for one hour. The cantilever deflection and OCP were recorded simultaneously; deflection values were converted to the corresponding surface stress values.[23] Light blue traces represent individual experiments and black traces represent the average stress for each applied potential. A gold-coated cantilever whose initial potential = −200 mV and −50 mV exhibit compressive surface stress values and when the initial potential is +200 mV, a tensile surface stress is observed. The initial value of the potential determines the magnitude and direction of the cantilever stress change upon release to the OCP condition. (B) Cantilever deflection was measured for clean and MCH-derivatized gold-coated cantilevers. The clean cantilever was held at V_{appl} = −200 mV for 2 minutes in TN buffer. The potential was subsequently switched to +200 mV. The same cantilever was then incubated in 1.0 mM MCH for 1 h. The amplitude of the stress change under the aforementioned V_{appl} is 8% of that observed for the cleaned gold-coated cantilever.

defined V_{appl} has a significant effect on the surface stress value because V_{appl} = ±200 mV on clean gold under the experimental electrolyte conditions leads to a surface stress change of 160 mN/m. Tightly packed MCH blocks ion adsorption and reduces the capacitance of the electrode.[20] Consistent with previous findings,[13] the amplitude of the surface stress change for the MCH-coated gold was greatly reduced (to 12 mN/m) from that observed for clean gold. The cleanliness of the gold surface is thus critical to obtaining large, reproducible signals.

To evaluate how controlling the surface charge density could be used in sensor applications, the effect of applying periodic square wave potentials to the functionalized gold-coated cantilever was studied. Cantilevers, clean gold-coated and

dx.doi.org/10.1021/la400975b | Langmuir 2013, 29, 9951−9957

gold-coated functionalized with 25-mer thiol-terminated oligonucleotides (probe-oligo) (Figure 3), were switched

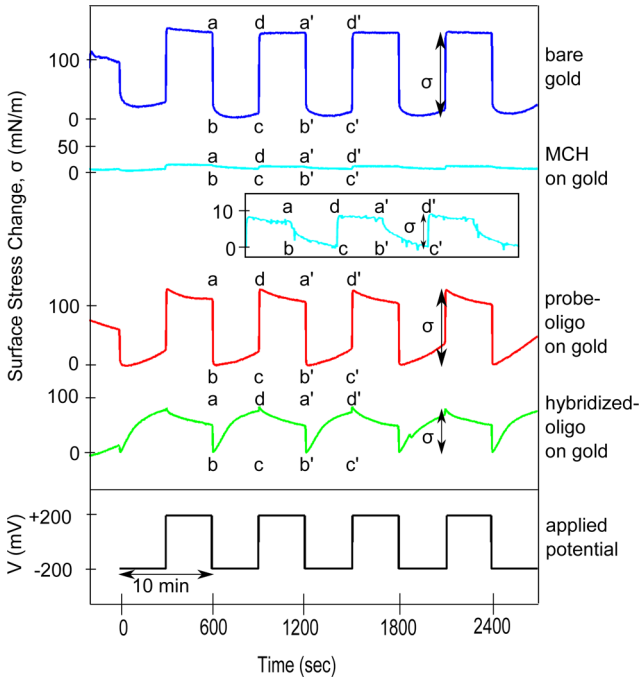

Figure 3. Electrochemically induced surface stress patterns of single- and double-stranded oligonucleotide-derivatized cantilever electrodes. The cantilever surface stress is measured in response to application of a square wave potential V_{appl} = ±200 mV with a 10 min interval (black trace). Segment a-b corresponds to switching of V_{appl} from +200 mV to −200 mV and c-d corresponds to switching of V_{appl} from −200 mV to +200 mV. Segments b-c and d-a' reflect the surface stress observed when V_{appl} is held at −200 mV and +200 mV respectively. Stress signals were observed for the clean gold-coated cantilever (blue trace) with σ = 160 mN/m, the gold-coated cantilever coated with MCH (light blue trace; see inset) with σ = 12 mN/m, the gold-coated cantilever functionalized with probe-oligo (red trace) with σ = 145 mN/m, and hybridized-oligo (green trace) with σ = 90 mN/m.

between ±200 mV with an interval time of 10 min. The clean gold-coated cantilever exhibited a surface stress time course that was in phase with the changes in the applied square wave potential, with a highly reproducible surface stress change of 160 mN/m being observed after the first potential cycle, persisting up to 20 cycles (Figure 3, dark-blue trace). The large magnitude of this signal makes it unnecessary to apply noise rejection methods such as the use of two cantilevers and differential deflection sensing. Functionalization of the cantilever with probe-oligo using a single-step functionalization procedure (Experimental Section) results in a stress pattern that is also in phase with the applied potential but undergoes a smaller stress change (145 mN/m) than does clean gold (Figure 3, red trace). Moreover, in contrast to the clean gold-coated cantilever, the surface stress of the probe-oligo cantilever has complex time-course features. For example, the initial compressive stress observed at V_{appl} = +200 mV undergoes a small but reproducible tensile change (Figure 3, red trace, d−a′). Similarly, the significant tensile stress observed at V_{appl} = −200 mV undergoes a compressive stress change with time (Figure 3, red trace, b−c). Because the time course of the surface stress may reflect dynamic changes in the orientation of the surface-tethered probe-oligo, we sought to determine whether the characteristic temporal features could be used to discriminate between single- and double- stranded oligonucleotides on the cantilever surface. The gold-coated cantilever functionalized with probe-oligo was thus incubated in a hybridization buffer containing the non-thiolated complementary oligonucleotide (target-oligo) to form thiolated double-stranded oligonucleotide (hybridized-oligo). Compared to the surface stress-time pattern observed for probe-oligo, hybridized-oligo shows greater tensile stress when V_{appl} = +200 mV (Figure 3, green trace, d−a′) and a larger compressive stress when V_{appl} = −200 mV (Figure 3, green trace, b−c). These results suggest that the stress patterns are influenced by increasing the charge density as well as by changing the orientation of the nucleic acid tethered to the surface cantilever surface.

To better understand how the quantity of probe-oligo at the gold surface affects the temporal features of the potential-dependent stress signal patterns, probe-oligo was tethered to the gold surface using an alternative multistep functionalization method (Experimental Section). The resulting cantilever deflection associated with each functionalization cycle was recorded (Figure 4A). As the quantity of probe-oligo bound to the surface increases with each successive functionalization procedure, the net stress change decreases. Both the compressive stress when V_{appl} = −200 mV and the tensile stress when V_{appl} = +200 mV increase. The stress changes observed on switching V_{appl} between +200 and −200 mV most likely derive from a competition between different adsorbates (Cl^-, surface-bound nucleotides, and buffer components) and their respective influences on surface stress. The principal ionic species present at the gold−solution interface have a potential-dependent affinity for the gold surface in the ±200 mV range.[25,26] Given that signal-generating adsorption events require unoccupied gold sites (Figures 2B and 3, light-blue trace), the decrease in the stress change is due to a lessening of the quantity of available gold caused by the functionalization of the probe-oligo (Figure 3, red trace). The observed compressive stress change when V_{appl} = −200 mV, for example, would arise from an increase in Cl^- adsorption at unoccupied gold in the presence of the probe-oligo. However, when V_{appl} = +200 mV, the probe-oligo is expected to have significant affinity for the gold surface and will be able to compete to some extent with Cl^- for gold adsorption sites, resulting in a tensile change in the surface stress.

The compressive stress changes observed when probe-oligo is tethered to the gold surface (Figure 3, red trace) and then subjected to periodic potential changes have been attributed to the reorientation of probe-oligo on the gold surface from a quasi-prone to a vertical state.[31,32] We postulate that the single-step functionalization process as described creates a random orientation of probe-oligo on the gold surface. The resulting probe-oligo is not effectively repelled from the gold surface at −200 mV. In contrast, the multistep functionalization process allows for electrochemical conditioning in some fashion, leading to an increased loading of probe-oligo as the tethered 25-mers are repetitively switched between prone and vertical orientations by the alternating periodic square wave potential. The ratio of the compressive stress change ($\sigma-$) to the stress amplitude (σ) in the case of the multistep functionalization process is dependent on the surface coverage of the probe-oligo (Figure 4B). The relatively small variation in stress changes compared to that of the cleaned gold-coated cantilevers in Figures 3 and 4A is due to the variation in the polycrystalline evaporated gold surface because the binding isotherm

dx.doi.org/10.1021/la400975b | Langmuir 2013, 29, 9951−9957

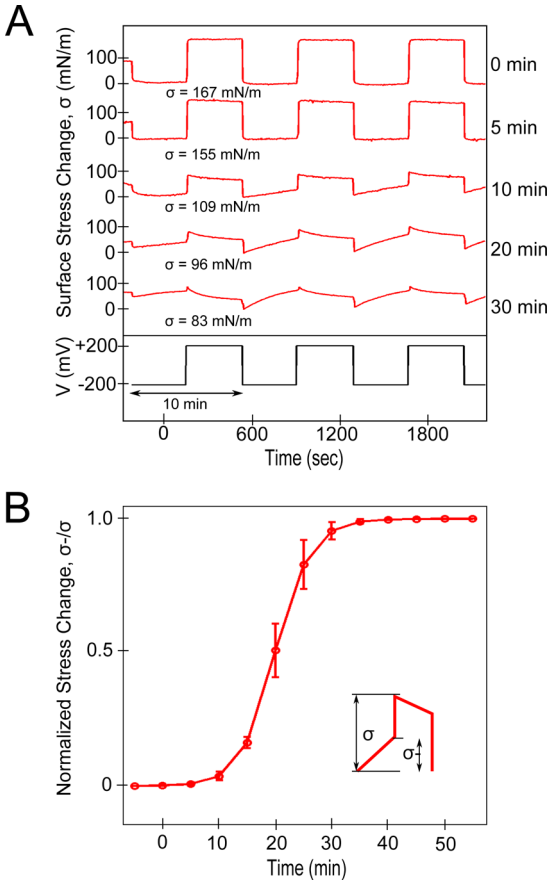

Figure 4. Surface stress time course change as a function of the oligonucleotide functionalization procedure. (A) Surface stress time course induced by multistep functionalization of the gold-coated cantilever with thiolated oligonucleotides. Stress change at baseline (top trace) and after 5 to 30 minutes functionalization periods (lower traces). The baseline stress signal (t = 0 minutes) shows a temporal surface stress pattern that is in-phase with the applied square wave potential (black trace) with σ = 167 mN/m. Following functionalization for 5 minutes the stress change exhibits a small compressive stress at V_{appl} = −200 mV and a tensile stress at V_{appl} = +200 mV, with σ = 155 mN/m. The surface stress signals observed following functionalization for 10, 20 or 30 minute periods. (B) The normalized compressive stress change (definition in inset) for V_{appl} = −200 mV measured as a function of functionalization time. The onset of compressive stress differed from one functionalization experiment to another, but the extent of surface coverage of probe-oligo can be readily controlled by monitoring the shape of the cantilever stress response as quantified by the normalized compressive stress change.

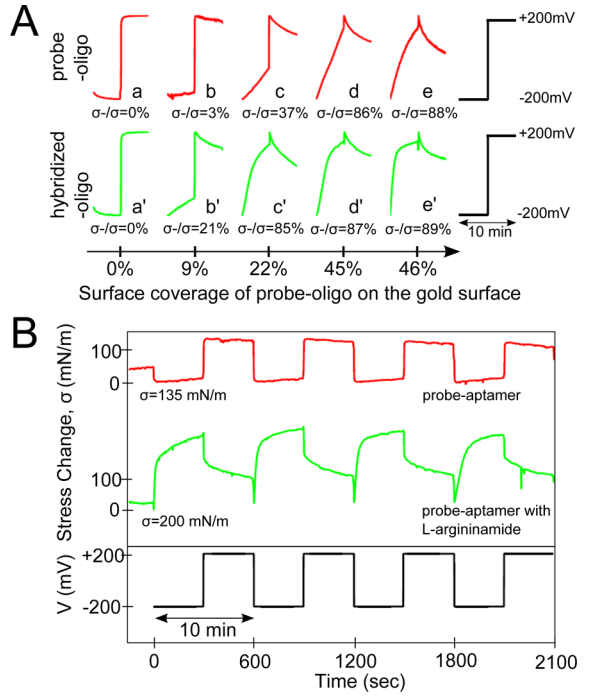

Figure 5. Characterization of surface stress time course changes in response to biomolecule capture. (A) Effect of surface coverage on surface stress time courses observed for probe-oligo and hybridized-oligo. Surface stress time courses are shown for probe-oligo (red trace) and hybridized-oligo (green trace) obtained at different values of the fractional coverage of the gold-coated cantilever [clean gold (a: probe-oligo, a′: hybridized-oligo); 9% surface coverage (b, b'); 22% surface coverage (c, c'); 45% surface coverage (d, d'); 46% surface coverage (e, e')]. The surface coverage was estimated electrochemically by backfilling with $Fc(CH_2)_{12}SH$ after each experiment[28] and coulometrically measuring the quantity of ferrocene derivative that has been chemisorbed. Surface stress values were measured during −200 mV and +200 mV applied potential regimes. (B) Detection of probe-aptamer binding cognate ligand with the electrochemically controlled cantilever sensor. The probe-aptamer was functionalized on a cleaned gold-coated cantilever and the surface stress signal was observed in response to an applied square wave potential (black trace), before (red trace) and after (green trace) incubation with 1.0 mM L-Arm solution for 30 minutes. The probe-aptamer surface coverage is 12% as determined by the $Fc(CH_2)_{12}SH$ method.

associated with each common crystal orientation is different to some extent.[29] The stress pattern changes following oligonucleotide hybridization (Figure 3, green trace) show a significant increase in compressive stress when V_{appl} = −200 mV. To use this stress pattern change as the basis for a biosensor, one needs to determine the optimum surface coverage of probe-oligo. To do so, clean gold-coated cantilevers were functionalized to different extents with probe-oligo, and the cantilever deflection was measured as a function of the periodic square wave potential (Figure 5A, red traces). Following incubation with target-oligo, the cantilever deflection was measured as a function of the periodic square wave potential (Figure 5A, green traces). Following the deflection measurements, each gold-coated cantilever was labeled with $Fc(CH_2)_{12}SH$ (Experimental Section), an electrochemically active reporter that can be used to determine the quantity of the gold surface that remains unfunctionalized.[28] Increasing the surface coverage of probe-oligo increases the magnitude of the compressive stress and significantly changes the shape of the surface stress−time curve (Figure 5A, green trace). The difference between the probe-oligo and hybridized-oligo signals is most apparent at intermediate rather than high coverage levels (e.g. Figure 5A, c and c′). The surface-tethered probe-oligo and hybridized-oligo differ in their respective total charge, their stiffness, and their orientation, each of which may be a factor in the observed stress profiles. For example, potential changes to more negative values have been shown to drive the hybridized-oligo away from the gold surface.[30,31] This would, in principle, allow for more Cl^- adsorption and a concomitant rise in compressive stress when V_{appl} = −200 mV. The hybridized-oligo, through its greater density of phosphate groups, would have more affinity for the gold surface at +200 mV than the single-strand oligonucleotide. Simulations by Rant and colleagues of equivalent systems also suggest that the lift-off rate of the hybridized oligo is greater

dx.doi.org/10.1021/la400975b | Langmuir 2013, 29, 9951−9957

than that of the single-strand oligonucleotide because of the greater chain stiffness in the former case.[32]

Whereas the effects of oligonucleotide charge, stiffness, and orientation on the observed stress change profiles are challenging to separate, our results suggest that other interactions involving a single-stranded oligonucleotide, such as the interaction between an oligonucleotide aptamer and its cognate ligand,[33,34] might also exhibit characteristic potential-dependent time courses. As a proof of principle, a 24-mer oligonucleotide aptamer (probe-aptamer) whose conformation changes following binding to L-argininamide (L-Arm) was studied. This binding results in increased stiffness and a looped structure of the probe-aptamer.[34] The gold-coated cantilever was thus functionalized with probe-aptamer to the extent that its surface stress response profile parallels that of the ca. 12% surface probe-oligo coverage situation (Figure 5B, red trace). Following incubation in an L-Arm solution (1.0 mM for 30 min), the cantilever deflection shows a clear change in its stress time course as a function of switching between +200 and −200 mV. The more rapid initial increase in compressive stress when the surface potential is held at −200 mV (Figure 5B, green trace) is attributed to the increased stiffness of the ligand-associated aptamer. The stress amplitude is also increased as a result of the surface-tethered aptamer-oligonucleotide wrapping around the L-Arm, thus making available an additional area of the gold surface for Cl^- adsorption.

CONCLUSIONS

The experiments reported here utilize oligonucleotides in solution as a prototypical molecular recognition system involving a number of charged species, each of which competes for surface sites. Electrochemical control offers the possibility to control the balance of ions close to and at the surface, generating large reproducible changes in the surface stress signal as a function of the applied potential. The temporal evolution of the surface stress signal of an oligonucleotide-derivatized gold surface, as a function of the applied potential, is dependent upon the surface loading of probe-oligo. This significantly changes the shape of the resultant periodic signal as well as its magnitude, providing a robust, information-rich read-out. Optimal coverage is not a densely packed monolayer because a large difference in the surface charge density associated with a specific binding event is sought. The result is a sensor that exhibits reproducible, characteristic signals upon (bio)chemical recognition events. This concept is demonstrated with a generic oligonucleotide aptamer sensor system, opening the possibility of microcantilever detection of DNA, proteins, and other small molecules.

AUTHOR INFORMATION

Corresponding Author

*E-mail: bruce.lennox@mcgill.ca.

Notes

The authors declare no competing financial interest.

ACKNOWLEDGMENTS

We gratefully acknowledge Mr. Brendan Pietrobon for fruitful discussions on electrochemical analysis, Mr. Haig Djambazian for fluorescent recording of oligonucleotide dynamics, Dr. Yoichi Miyahara for electrical and optical devices for cantilever deflection recordings, and Dr. James Hedberg for generating Figure 1A. Y.N. thanks Genome Canada and Genome Quebec for financial support. Funding for this research was provided by an Emerging Team Grant in Regenerative Medicine and Nanomedicine from the Canadian Institutes of Health Research (CIHR) and Discovery Grants from the Natural Sciences and Engineering Research Council of Canada.

ABBREVIATIONS

TN buffer, Tris-HCl NaCl buffer; TE buffer, Tris-HCl EDTA buffer; PSD, position-sensitive detector; MCH, 6-mercapto-1-hexanol; probe-oligo, thiolated single-strand oligonucleotide; hybridized-oligo, thiolated double-strand oligonucleotide; target-oligo, non-thiolated complementary oligonucleotide for probe-oligo; DTT, dithiothreitol; ferrocenyl C12-thiol, 12-ferrocenyl-1-dodecanethiol; L-Arm, L-argininamide dihydrochloride; OCP, open circuit potential; PZC, potential of zero charge

REFERENCES

(1) Berger, R.; Delamarche, E.; Lang, H. P.; Gerber, C.; Gimzewski, J. K.; Meyer, E.; Guntherodt, H. J. Surface stress in the self-assembly of alkanethiols on gold. *Science* **1997**, *276*, 2021−2024.

(2) Fritz, J.; Baller, M. K.; Lang, H. P.; Rothuizen, H.; Vettiger, P.; Meyer, E.; Guntherodt, H. J.; Gerber, C.; Gimzewski, J. K. Translating biomolecular recognition into nanomechanics. *Science* **2000**, *288*, 316−318.

(3) Braun, T.; Ghatkesar, M. K.; Backmann, N.; Grange, W.; Boulanger, P.; Letellier, L.; Lang, H. P.; Bietsch, A.; Gerber, C.; Hegner, M. Quantitative time-resolved measurement of membrane protein-ligand interactions using microcantilever array sensors. *Nat. Nanotechnol.* **2009**, *4*, 179−185.

(4) Braun, T.; Backmann, N.; Vogtli, M.; Bietsch, A.; Engel, A.; Lang, H. P.; Gerber, C.; Hegner, M. Conformational change of bacteriorhodopsin quantitatively monitored by microcantilever sensors. *Biophys. J.* **2006**, *90*, 2970−2977.

(5) McKendry, R.; Zhang, J.; Arntz, Y.; Strunz, T.; Hegner, M.; Lang, H. P.; Baller, M. K.; Certa, U.; Meyer, E.; Guntherodt, H. J.; Gerber, C. Multiple label-free biodetection and quantitative DNA-binding assays on a nanomechanical cantilever array. *Proc. Natl. Acad. Sci. U.S.A.* **2002**, *99*, 9783−9788.

(6) Arlett, J. L.; Myers, E. B.; Roukes, M. L. Comparative advantages of mechanical biosensors. *Nat. Nanotechnol.* **2011**, *6*, 203−215.

(7) Stern, E.; Klemic, J. F.; Routenberg, D. A.; Wyrembak, P. N.; Turner-Evans, D. B.; Hamilton, A. D.; LaVan, D. A.; Fahmy, T. M.; Reed, M. A. Label-free immunodetection with CMOS-compatible semiconducting nanowires. *Nature* **2007**, *445*, 519−522.

(8) Stern, E.; Wagner, R.; Sigworth, F. J.; Breaker, R.; Fahmy, T. M.; Reed, M. A. Importance of the Debye screening length on nanowire field effect transistor sensors. *Nano Lett.* **2007**, *7*, 3405−3409.

(9) Ibach, H. The role of surface stress in reconstruction, epitaxial growth and stabilization of mesoscopic structures. *Surf. Sci. Rep.* **1997**, *29*, 195−263.

(10) Haiss, W. Surface stress of clean and adsorbate-covered solids. *Rep. Prog. Phys.* **2001**, *64*, 591−648.

(11) Smetanin, M.; Viswanath, R. N.; Kramer, D.; Beckmann, D.; Koch, T.; Kibler, L. A.; Kolb, D. M.; Weissmuller, J. Surface stress-charge response of a (111)-textured gold electrode under conditions of weak ion adsorption. *Langmuir* **2008**, *24*, 8561−8567.

(12) Watari, M.; Galbraith, J.; Lang, H.-P.; Sousa, M.; Hegner, M.; Gerber, Ch.; Horton, M. A.; McKendry, R. A. Investigating the molecular mechanisms of in-plane mechanochemistry on cantilever arrays. *J. Am. Chem. Soc.* **2007**, *129*, 601−609.

(13) Godin, M.; Tabard-Cossa, V.; Miyahara, Y.; Monga, T.; Williams, P. J.; Beaulieu, L. Y.; Lennox, R. B.; Grutter, P. Cantilever-based sensing: the origin of surface stress and optimization strategies. *Nanotechnology* **2010**, *21*, 75501.

(14) Wu, G.; Ji, H.; Hansen, K.; Thundat, T.; Datar, R.; Cote, R.; Hagan, M. F.; Chakraborty, A. K.; Majumdar, A. Origin of

nanomechanical cantilever motion generated from biomolecular interactions. *Proc. Natl. Acad. Sci. U.S.A.* **2001**, *98*, 1560−1564.
(15) Lang, H. P.; Hegner, M.; Gerber, C. Cantilever array sensors. *Mater. Today* **2005**, *8*, 30−36.
(16) Boisen, A.; Thundat, T. Design & fabrication of cantilever array biosensors. *Mater. Today* **2009**, *12*, 32−38.
(17) Haiss, W.; Nichols, R. J.; Sass, J. K.; Charle, K. P. Linear correlation between surface stress and surface charge in anion adsorption on Au(111). *J. Electroanal. Chem.* **1998**, *452*, 199−202.
(18) Tabard-Cossa, V.; Godin, M.; Burgess, I. J.; Monga, T.; Lennox, R. B.; Grutter, P. Microcantilever-based sensors: effect of morphology, adhesion, and cleanliness of the sensing surface on surface stress. *Anal. Chem.* **2007**, *79*, 8136−8143.
(19) Tabard-Cossa, V.; Godin, M.; Beaulieu, L. Y.; Grutter, P. A differential microcantilever-based system for measuring surface stress changes induced by electrochemical reactions. *Sens. Actuators, B* **2005**, *107*, 233−241.
(20) (a) Steel, A. B.; Herne, T. M.; Tarlov, M. J. Electrochemical Quantitation of DNA Immobilized on Gold. *Anal. Chem.* **1998**, *70*, 4670−4677. (b) Lee, D.; Thundat, T.; Jeon, S. Electromechanical identification of molecules adsorbed on microcantilevers. *Sens. Actuators, B* **2007**, *124*, 143−146.
(21) Pan, H.; Xu, Y.; Wu, S.; Zhang, B.; Tang, J. Molecular interactions in self-assembly monolayers on gold-coated microcantilever electrodes. *Nanotechnology* **2011**, *22*, 225503.
(22) Stoney, G. G. The tension of metallic films deposited by electrolysis. *Proc. R. Soc. London, Ser. A* **1909**, *82*, 172−175.
(23) Sader, J. E.; Chon, J. W. M.; Mulvaney, P. Calibration of rectangular atomic force microscope cantilevers. *Rev. Sci. Instrum.* **1999**, *70*, 3967−3969.
(24) Godin, M.; Tabard-Cossa, V.; Grutter, P.; Williams, P. Quantitative surface stress measurements using a microcantilever. *Appl. Phys. Lett.* **2001**, *79*, 551−553.
(25) Lipkowski, J.; Shi, Z. C.; Chen, A. C.; Pettinger, B.; Bilger, C. Ionic adsorption at the Au(111) electrode. *Electrochim. Acta* **1998**, *43*, 2875−2888.
(26) Hinnen, C.; Rousseau, A.; Parsons, R.; Reynaud, J. A. Comparison Between The Behaviour of Native and Denatured DNA at Mercury and Gold Electrodes by Capacity measurements and Cyclic Voltammetry. *J. Electroanal. Chem.* **1981**, *125*, 193−203.
(27) Harada, K.; Frankel, A. D. Identification of two novel arginine binding DNAs. *EMBO J.* **1995**, *14*, 5798−811.
(28) Lee, L. Y. S.; Lennox, R. B. Ferrocenylalkylthiolate labeling of defects in alkylthiol self-assembled monolayers on gold. *Phys. Chem. Chem. Phys.* **2007**, *9*, 1013−1020.
(29) Hamelin, A.; Bellier, J. P. Role de l'orientation cristallographique dans l'adsorption de l'ion chlorure sur l'or. I-zone [110]. *J. Electroanal. Chem. Interfacial Electrochem.* **1973**, *41*, 179−192.
(30) Kelley, S. O.; Barton, J. K.; Jackson, N. M.; McPherson, L. D.; Potter, A. B.; Spain, E. M.; Allen, M. J.; Hill, M. G. Orienting DNA helices on gold using applied electric fields. *Langmuir* **1998**, *14*, 6781−6784.
(31) Rant, U.; Arinaga, K.; Fujita, S.; Yokoyama, N.; Abstreiter, G.; Tornow, M. Dynamic electrical switching of DNA layers on a metal surface. *Nano Lett.* **2004**, *4*, 2441−2445.
(32) Rant, U.; Arinaga, K.; Tornow, M.; Kim, Y. W.; Netz, R. R.; Fujita, S.; Yokoyama, N.; Abstreiter, G. Dissimilar kinetics behavior of electrically manipulated single- and double-stranded DNA tethered to a gold surface. *Biophys. J.* **2006**, *90*, 3666−3671.
(33) Hamaguchi, N.; Ellington, A.; Stanton, M. Aptamer beacons for the direct detection of proteins. *Anal. Biochem.* **2001**, *294*, 126−131.
(34) Guo, X.; Liu, Z.; Liu, S.; Bentzley, C. M.; Bruist, M. F. Structural features of the L-argininamide-binding DNA aptamer studied with ESI-FTMS. *Anal. Chem.* **2006**, *78*, 7259−7266.